Transfinite Interpolation Technique for P-version of F.E.M.

초유한 보간법에 의한 P-version 유한요소해법

우 광 성*
Woo, Kwang Sung

Abstract

In the h-version of F.E.M., all piecewisely smooth curved boundaries can be approximated by a sufficient number of straight-sided elements. However, in the p-version the size of the element is usually large and hence the probability of distortions is more. An attempt has been made to generate a curved boundary by using a transfinite interpolation technique to avoid the discretization errors. In the following sections, it will be shown how to construct transfinite interpolants both in h-version and in p-version over polygonal and nonpolygonal regions. Three numerical tests are shown to validate the applicability and superior capability of transfinite interpolation technique.

요 약

h-version 유한요소에서 평활 곡선경계는 충분한 갯수의 직선경계에 의해 근사될 수 있다. 그러나, 일반적으로 곡선경계가 충분하지 않은 갯수의 직선변을 갖는 다각형요소, 또는 곡선요소등에 의한 사상이 정확하지 않을 경우 해가 수렴되지 않을 뿐만아니라 특히, 곡면에 수직방향의 응력은 다른 방향의 응력요소에 비해 수렴속도가 늦거나 틀린 해를 보여 준다. 한편, p-version 유한요소는 사용되는 요소의 크기가 클 뿐아니라 변형되는 정도가 크므로 이러한 이산오차를 피하기 위해 초유한 보간기법이 제안되어 정확한 사상을 하게 된다. 본 연구에서는 직선경계는 물론 곡선경계에 초유한 사상을 h-version과 p-version에 적용하는 방법과 이에 필요한 초유한 보간자를 유도하여 세 문제의 예제를 통해 그 적용성과 우월성을 보이고자 한다.

1. Introduction

The conventional finite element method involves the partitioning of a polygonal domain Ω into rectangular and/or triangular elements. Quite often, however, a structural engineer is faced with a boundary value problem over a nonpolygonal domain Ω. The early approaches in finite element modeling required that the boundary, $\partial\Omega$, of Ω be approximated by a polygonal arc. Obviously, the accuracy of the F.E.M. is limited by the accuracy of the polygonal approximation to $\partial\Omega$. At worst, the convergence of the F.E.M. may be destroyed if boundary conditions are not handled properly. The Babuska paradox[1] describes an error asssociated with modeling a curved boundary by straight-sided elements. Thus, if a mesh with a regular polygon as its boundary serves to model a circular region, a refinement of the

* 정회원, 전남대학교, 토목공학과, 조교수

이 논문에 대한 토론을 1992년 6월 30일까지 본 학회에 보내주시면 1992년 12월호에 그 결과를 게재하겠습니다.

mesh causes the polygon to have more sides and to converge to a circle. We would then expect stresses to converge to values that are exact for the circular region. In reality the strains ε_n and stresses σ_n normal to the boundary converge to wrong values. To avoid this error, elements with curved edges should be used. In order to better conform to curved geometries and thus reduce discretization error, curved finite elements have been widely applied in recent years. Krathammer,[1] Irons and Zienkiewicz[9] have developed various curved parametric finite elements which tend to circumvent the above dilemma in the case of certain shapes of the curved boundary. For mathematical convenience, in general, the shape functions are defined on standard domains(e.g. triangles, squares, cubes etc.) and are mapped into real domain by suitable coordinate trans-formations. The most commonly used mappings are linear and quadratic parametric mappings does not introduce large distortions in the h-version, and all piecewise smooth boundaries can be approximated by a sufficient number of piecewisely quadratic polynomials. In the p-version, however, the size of the element is usually large and hence the probability of distortions is more, especially if higher order parametric mapping is used, unless the boundary of an element is represented by a polynominal in the parametric form. In the case of nonpolygonal boundaries, like circles and ellipses, parametric mapping may not work at all.[2,3] In the case of the proposed element, only the four corners of an quadratic element will be referred to mapping from the standard to the real domain. It is therefore necessary to find the mapping function which will exactly map the standard element to the sides of the real element including the four corner nodes by making use of the exact geometric parameters of the curved boundary.[4] In this study, an attempt has been made to generate a curved boundary by using a transfinite interpolation technique. This technique has been discussed in detail by Gordon and Hall.[2,3] So, this paper represents an approach to apply the transfinite interpolation technique based on p-version of finite element concepts to several structural problems. Also, the shape functions used in this study are based on Integrals of Legendre polynomials.

2. Transfinite Interpolation Technique

The term 'transfinite' is used to describe a general class of interpolation schemes. Unlike the classical methods of higher dimensional interpolation which match the primitive function f at a finite number of distinct points, these methods match f at a non-denumerable(transfinite) number of points. Such a transfinite interpolatory mapping of a domain such as the unit square onto the domain of interest Ω introduces a natural curvilinear coordinate system on Ω. In other words, we refer to the class of interpolation formula as being transfinite, since their precision sets(i.e., the set of points in the domain of the independent variables s, t on which the interpolant matches the original function) are non-denumerable. In particular, the transfinite schemes[5,6] to be considered are of the type referred to as 'blend-function methods'. Let f be a continuous function of two independent variables with domain L; [0,h] x[0, h] in the s-t plane as shown in Fig. 1. By a projector P, we mean a linear operator from the linear space T of all continuous bivariate function f, with domain L, onto a subspace of

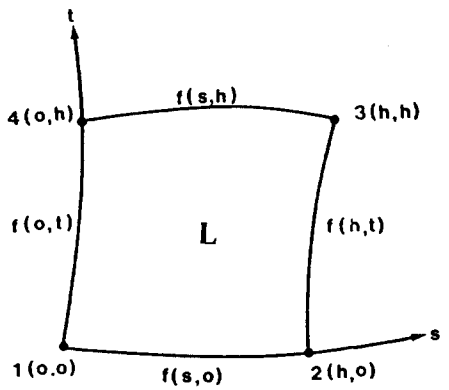

Fig. 1 Domain L in the s-t plane

functions. For example, if the operator P_s is defined by the formula :

$$P_s[f]=(1-s/h)\cdot f(0,t)+(s/h)\cdot f(h,t) \qquad (1)$$

It can be expressed by the general form as follows :

$$P_s[f]=\sum_{i=0}^{m} f(s_i,\ t)\cdot \Phi_i(s) \qquad (2)$$

where $0=s_0<s_1<\cdots<s_m=h$ and

$$\Phi_i(s)=\prod_{j\neq i}(s-s_j)\ /\ \prod_{j\neq i}(s_i-s_j),\ \ 0\leq i\leq m \qquad (3)$$

are the fundamental functions for Lagrange polynomial interpolations. For completeness and later reference, we display the analogous formula for P_t :

$$P_t[f]=\sum_{j=0}^{n} f(s,\ t_j)\cdot \psi_j(t) \qquad (4)$$

where $0=t_0<t_1<\cdots<t_n=h$ and

$$\psi_j(t)=\prod_{i\neq j}(t-t_i)\ /\ \prod_{i\neq j}(t_j-t_i),\ 0\leq j\leq n \qquad (5)$$

There is a way to compound the projectors P_s and P_t by using Boolean sum.

$$P_s\oplus P_t\equiv P_s+P_t-P_sP_t \qquad (6)$$

3. Transfinite Interpolants in P-version

The transfinite interpolants for curved boundary can be achieved by constructing blend mapping functions. First, each side of the element with arbitrary boundaries is defined by parametric equations in terms of standard coordinates shown in Fig.2. The transfinite interpolants for each side of the element are expressed in Eq. (7).

$$\begin{aligned}
&\text{Side 1} && \begin{cases} x=x_1(\xi) \\ y=y_1(\xi) \end{cases} \\
&\text{Side 2} && \begin{cases} x=x_2(\eta) \\ y=y_2(\eta) \end{cases} \\
&\text{Side 3} && \begin{cases} x=x_3(\xi) \\ y=y_3(\xi) \end{cases} \\
&\text{Side 4} && \begin{cases} x=x_4(\eta) \\ y=y_4(\eta) \end{cases}
\end{aligned} \qquad (7)$$

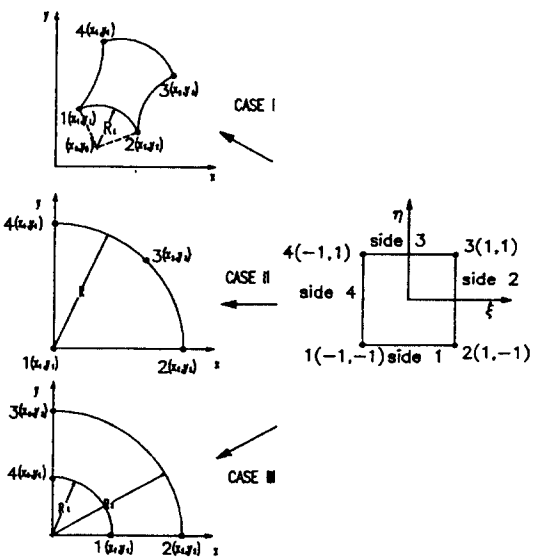

Fig.2 Transfinite Interpolants From Standard Domain to Real Domain in the plane

The suitable transfinite interpolants of each side have been derived for the plane domain. It may be noted that for Case Ⅰ, the edge 1−2 is circular with radius R_1 and the other three edges are arbitrary. In Case Ⅱ, the node 3 is the midpoint of the circular arc 2−4, and the edges 1−2 and 4−1 are straight. But, in Case Ⅲ, the edges 1−4 and 2−3 are circular arcs with radius R_1 and R_2, whereas, the edges 1−2 and 3−4 are straight. In Case Ⅰ, the suitable tranfinite interpolants for side 1, which are function of ξ, is derived for demonstration.

$$x_1(\xi)=x_0+R_1\cos\left(\theta_1\frac{1-\xi}{2}+\theta_2\frac{1+\xi}{2}\right)$$

$$y_1(\xi)=y_0+R_1\sin\left(\theta_1\frac{1-\xi}{2}+\theta_2\frac{1+\xi}{2}\right) \quad (8)$$

The rest of transfinite interpolants in Fig.2, which are function of ξ and η, for Case Ⅱ and Case Ⅲ can be derived like Eq.(7).

For Side 1($-1\leq\xi\leq1$)

Case Ⅱ, Case Ⅲ

$$x_1(\xi)=x_1\frac{1-\xi}{2}+x_2\frac{1+\xi}{2}$$

$$y_1(\xi)=y_1\frac{1-\xi}{2}+y_2\frac{1+\xi}{2} \quad (9)$$

For Side 2($-1\leq\eta\leq1$)

Case Ⅱ

$$x_2(\eta)=x_1+R\cos\left(\theta_2\frac{1-\eta}{2}+\theta_3\frac{1+\eta}{2}\right)$$

$$y_2(\eta)=y_1+R\sin\left(\theta_2\frac{1-\eta}{2}+\theta_3\frac{1+\eta}{2}\right)$$

Case Ⅲ

$$x_2(\eta)=R_2\cos\left(\theta_2\frac{1-\eta}{2}+\theta_3\frac{1+\eta}{2}\right)$$

$$y_2(\eta)=R_2\sin\left(\theta_2\frac{1-\eta}{2}+\theta_3\frac{1+\eta}{2}\right) \quad (10)$$

For Side 3($-1\leq\xi\leq1$)

Case Ⅱ

$$x_3(\xi)=x_1+R\cos\left(\theta_3\frac{1+\xi}{2}+\theta_4\frac{1-\xi}{2}\right)$$

$$y_3(\xi)=y_1+R\sin\left(\theta_3\frac{1+\xi}{2}+\theta_4\frac{1-\xi}{2}\right)$$

Case Ⅲ

$$x_3(\xi)=x_3\frac{1+\xi}{2}+x_4\frac{1-\xi}{2}$$

$$y_3(\xi)=y_3\frac{1+\xi}{2}+y_4\frac{1-\xi}{2} \quad (11)$$

For Side 4($-1\leq\eta\leq1$)

Case Ⅱ

$$x_4(\eta)=x_4\frac{1+\eta}{2}+x_1\frac{1-\eta}{2}$$

$$y_4(\eta)=y_4\frac{1+\eta}{2}+y_1\frac{1-\eta}{2}$$

Case Ⅲ

$$x_4(\eta)=R_1\cos\left(\theta_1\frac{1-\eta}{2}+\theta_4\frac{1+\eta}{2}\right)$$

$$y_4(\eta)=R_1\sin\left(\theta_1\frac{1-\eta}{2}+\theta_4\frac{1+\eta}{2}\right) \quad (12)$$

The individual mapping functions are blended with the opposite sides of the element by means of projectors $(\eta-1)/2$, $(\xi+1)/2$, $(\eta+1)/2$, $(\xi-1)/2$. In the process, the mapping functions take the following form in Eq.(6) by Boolean sum.

$$X=x_1(\xi)(1-\eta)/2+x_3(\xi)(1+\eta)/2+x_2(\eta)(1+\xi)/2+x_4(\eta)(1-\xi)/2-x_1(1-\xi)(1-\eta)/4-x_2(1+\xi)(1-\eta)/4-x_3(1+\xi)(1+\eta)/4-x_4(1-\xi)(1+\eta)/4 \quad (13)$$

$$Y=y_1(\xi)(1-\eta)/2+y_3(\xi)(1+\eta)/2+y_2(\eta)(1+\xi)/2+y_4(\eta)(1-\xi)/2-y_1(1-\xi)(1-\eta)/4-y_2(1+\xi)(1-\eta)/4-x_3(1+\xi)(1+\eta)/4-x_4(1-\xi)(1+\eta)/4$$

4. Numerical Tests

4.1 Circular Plate

One quarter of a circular plate of radius, R, subjected to a central concentrated load shown in Fig.3, $p=1.0$ lb(or uniformly distributed load $q_0=1.0\,psi$), is modeled with one p−version

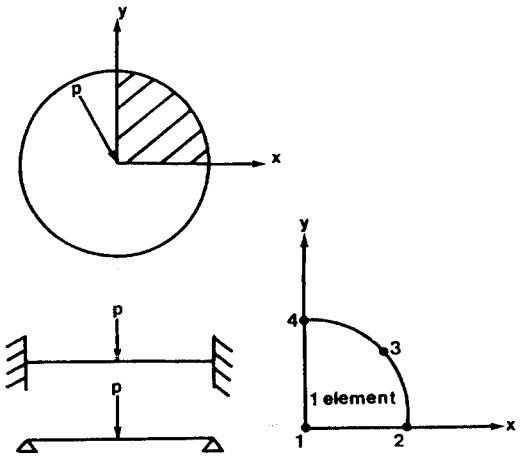

Fig.3 Centrally Loaded Circular Plate with Clamped and Simply Supported Outer Edge.

element which maps the circular boundary by transfinite interpolation technique as discussed earlier. The problem data are R=2.0in, Poisson's ratio=0.3, thickness=0.01*in* and s modulus is 0.1092×10^{8} $1b/in^{2}$. This problem has been studied by using the heterosis, Lagrange, and serendipity elements, but the singularity gives rise to almost identical oscillatory patterns for Lagrange and serendipity elements. However, the 48-element mesh of heterosis type proposed by Hughes was emloyed to get the same degree of accuracy as Timoshenko's solution. On the other hand, one-element p-version model shows excellent agreement with Timoshenko's as p-level is increased up to 8. It may be noted that the maximum deflection at the center of a circular plate by p-version model is relatively greater than Timoshenko's value because the finite element used includes the effect of transverse shear deformations. The results by p-version of the finite element method are presented in Table 1.

Table 1. Max deflection at the center for clamped and S.S. (simply supported) circular plate

P-Level	w_{max}(Uniform Load)		w_{max}(Point Load)	
P=6	0.23680	1.01902	0.06850	0.19558
P=7	0.24511	1.02410	0.07594	0.19939
P=8	0.24978	1.02572	0.07769	0.20151
P=9	0.25011	1.02806	0.07856	0.20264
P=10	0.25026	1.03997	0.07906	0.20542
Timoshenko	0.25000	1.01923	0.07958	0.20200

4.2 Thick-Walled Cylinder

The thick-walled cylinder under a unit internal pressure is shown in Fig.4. The geometry of the problem is the same as an example of SAP90 verification manual. For the pressure loading, the results obtained by theoretical and SAP90 analyses with 45 ASOLID 9-node elements for the radial displacement and stresses at the inner surface are compared with the results by one element p-version model with different p-levels in Figs. 5,6 and 7. In general, errors in normal stress σ_n can be of the order of the tangential stress by Babuska's paradox. However, it is shown that one element p-version model can avoid this discretization errors due to the curved boundary from Fig.6 and 7.

4.3 Circular Hole In A Rectangular Panel

In this problem, the effects of extreme aspect ratios and non polynomial mapping have been investigated. The stress concentration factors at the neck for r/b (radius to half width ratio) ranging 0.001 to 0.99 are compared with the experimental solutions by Nisida, Howland[7] etc. and numerical solutions from NASTRAN 334-element model and FIESTA-2D[8] three element model. FIESTA-2D is a commercial code based on p-version of the finite element method. A typical h-version mesh of NASTRAN and the p-ver-

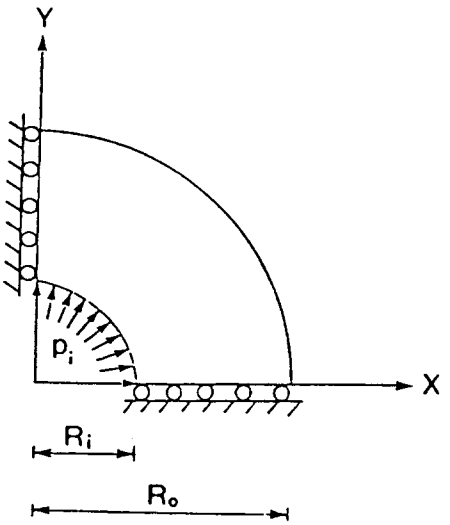

INNER RADIUS	= 3.0
OUTER RADIUS	= 9.0
MODULUS OF ELASTICITY	= 10.0×10^5
POISSON'S RATIO	= 0.3

Fig.4 Configuration and one element p-version model of thick-walled cylinder

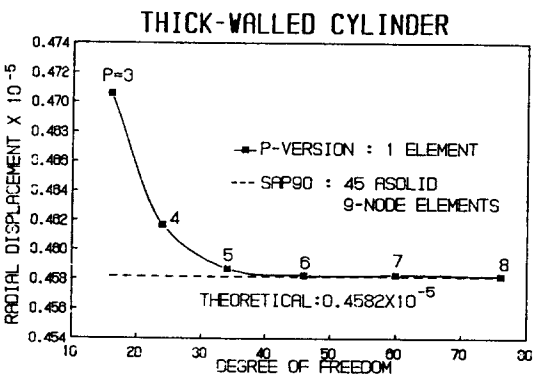

Fig.5 Convergence of radial displacement

sion mesh are shown in Fig.8. Of interest is the maximum stress. The maximum stress, computed directly from the finite element solution using the three-element mesh with the polynomial degree ranging from 1 to 8 and r/b=0.2, is shown in Fig.9. It is seen that the

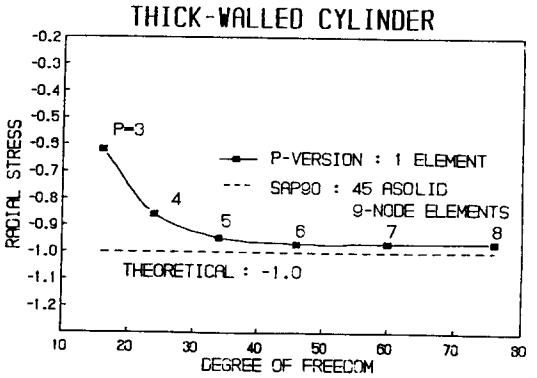

Fig.6 Covergence of radial stress

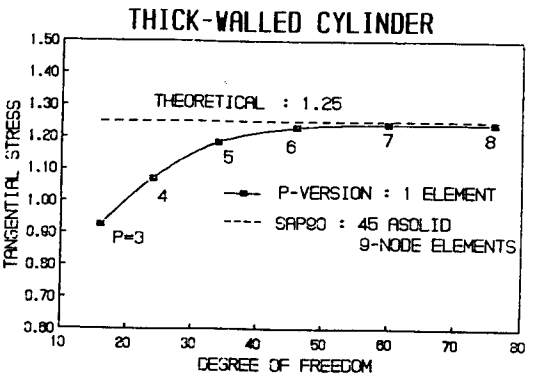

Fig.7 Covergence of tangential stress

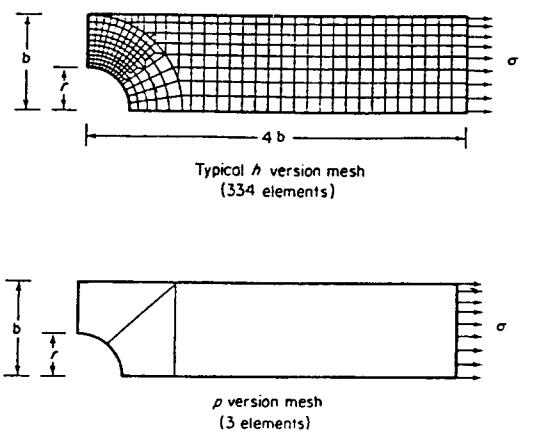

Fig.8 Quarter model of a rectangular panel with a circular hole

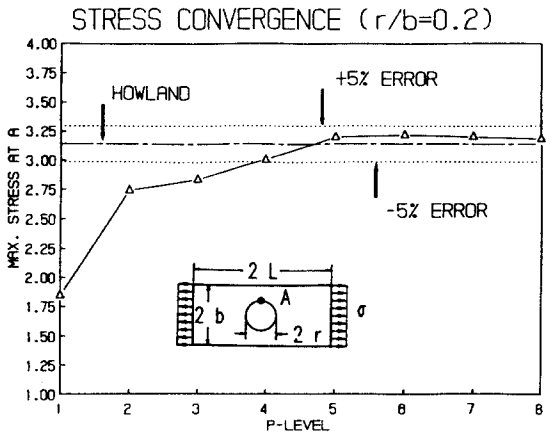

Fig.9 Maximum stress at point A when r/ b=0.2

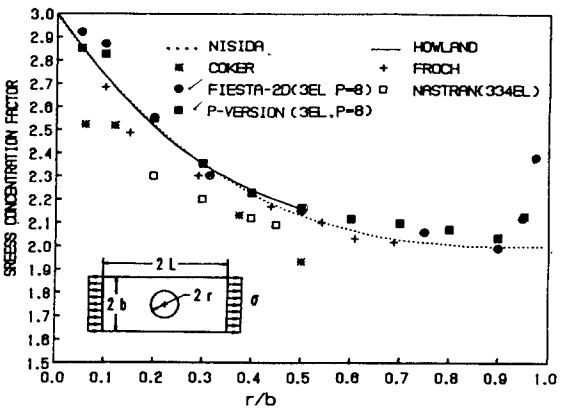

Fig.10 Stress concentration factor as function of r/ b

r5.end

stress value is well within the 5 percent relative error range for p=4 to 8 compared with Howland's experimental solution. The fact that the p-version tolerates large aspect ratio is illustrated in Fig.10. Using the same three-element mesh as shown in Fig.8, the stress concentration factors are computed for a wide range of r /b ratios.

5. Conclusions

It has been established a class of transfinite interpolation formula based on the use of blend functions. It may be noted that in the case of both triangular and quadrilateral elements, one or more of the boundaries may be curved, in which case mapping from standard elements becomes more important. Moreover, the concepts of exact mapping in the p-version can be stressed on since large elements are used. The p-version element based on transfinite interpolation technique with Integrals of Legendre polynomials is found to avoid the discretization errors due to the curved boundaries from three numerical examples.

6. References

(1) T. Krathammer, "Accuracy of the Finite Element Method Near a Curved Boundary", CompSt., Vol.10, No.6, pp.921-929, 1979.

(2) W.J.Gordon and C.A. Hall, "Transfinite Element Method: Blending-Function Interpolation over Arbitary Curved Element Domains", Numer. Math.21, 109-129, 1973.

(3) W.J.Gordon and C.A. Hall, "Construction of Curvilinear Coordinate Systems and Applications to Mesh Generation", Int. J. Numer. Meth. Engng., Vol.7, pp.461-477, 1973.

(4) S.H.Lo, "Finite element mesh generation over curved surfaces", Comput. Struct., Vol.29, pp.731-742, 1988.

(5) K.K.Tamma and S.B.Railkar, "Transfinite element methodology to towards a unified thermal structural analysis", Comput. Struct. Vol.25, pp.649-660, 1987.

(6) K.V.R. Vardhani and N.S. Prasad, "Mesh generation for spherical and conical surfaces using transfinite interpolation",

Comput. Struct., Vol.32, No.6, 18, 1359-1362, 1989.
(7) 中原一郎, "應力集中", 養賢堂版, 1984.
(8) B.A. Szabo, "Estimation and Control of Error Based on p-Convergence", Accuracy Estimates and Adaptive Refinements in Finite Element Computations, Edited By I. Babuska, O.C. Zienkiewicz etc., John Wiley & Sons Ltd., 1986.
(9) O.C. Zienkiewicz and D.V. Phillips, "An automatic mesh generation scheme for plane and curved surfaces by isoparametric coordinates", Int. J. Numer. Meth. Engng. 3, pp.519-529, 1971.

(접수일자 1991. 9. 28)